

# Bundle strength of polyester fibers determined using a series-parallel combination model

KEE HWAN CHO, SUNG HOON JEONG

*Division of Chemical Engineering, College of Engineering, Hanyang University, Seoul Korea*

*E-mail: shjeong@hanyang.ac.kr*

This paper describes the bundle strengths of PET filaments from a statistical point of view. A bundle is an arrangement of a number of filaments. We applied the weakest-link theory and probabilistic load-sharing rules to estimate the bundle strength from the breaking strength data of PET filaments. We analyzed the breaking behavior of 12 filament bundles according to their length and number of filaments and compared the breaking behavior of a prepared specimen yarn with that of a commercial PET filament yarn. The breaking strength of the PET filaments, which we tested using a MANTIS<sup>®</sup> tester, was compared with that of the actual yarn. We compared the actual tested values obtained by INSTRON<sup>®</sup> with the expected values, which we calculated from the MANTIS<sup>®</sup> data by using Peirce's theory and Knox's hazard function. The key effects that determine the actual random breakage behavior of a bundle include not only the load-sharing rules in the constituent filaments but also the slippage and friction between adjacent filaments, the appearance of which we distinguished especially in the bundle consisting of a large number of filaments and in small-denier filaments. The PET filaments were better approximated when using the Peirce's weakest-link theory than they were by Knox's hazard function. In a series-parallel model, we found that the number of parallel filaments and their load-sharing behavior had larger effects on the bundle strength than did the weakest-link effects of continuous elements. © 2005 Springer Science + Business Media, Inc.

## 1. Introduction

Although the tensile strengths of textile materials are determined by those of their components, it is well known that the tensile strength of fiber bundles and yarns is not predicted accurately from that of its single fibers by the use of simple averaging methods or mathematical calculations, because of variations in their strength. Textile fibers are not uniform: their composition and fineness both vary from one fiber to another in a sample and along the length of each fiber; consequently, their tensile properties are also variable. Therefore, when determining the tensile strength of a textile fiber, it is necessary to approach the problem through statistical concepts because of these variations [1–13]. First, we could consider the weakest-link effect on the tensile strength of the filament. The weakest-link effect is concerned with the effect of variability on strength [1]. For a filament under a given tension, the stress will vary from place to place and will follow the variations of the cross-section. At each point, the specific stress will be given by the tension divided by the linear density at that point. As a consequence of the variation of stress, the strain will also vary from place to place. Second, if we test a number of filaments together, i.e., a bundle of filaments, rather than testing a single filament, the form of the specimen has

a considerable influence on the result of the strength test. Practical cases are usually complicated and difficult to formulate mathematically. The simple examples given by Peirce may be used to evaluate the composite-specimen effects. The composite type given by Peirce may be classified according to the gripping, original length, loading, and slipping. The test method will be different according to each composite specimen type. Finally, the load-sharing rules should be determined; these values can be analyzed from load-elongation curves of the bundles [14–21]. The load-sharing rules may be changed according to the composite-specimen effect. For example, if filaments are gripped at the ends, of equal original length, and of uniform breaking extension, all of the filaments will break together, and the breaking load of the composite specimen will be equal to the sum of the breaking loads of the filaments.

In this study, we considered filaments to be composed of an element and a bundle to be an arrangement of a number of filaments. We discuss statistical approaches to determine the parallel-bundle breakage mechanism from data from single-filaments of PET. We prepared twelve sets of composite specimens having different lengths from 262d/12f PET yarn, and then their normality and distribution

identity were tested using the MINITAB® statistics package. We applied generally accepted series models to the tested results and evaluated their applicability to the analysis of PET filament yarn. The random breakage model was considered for arrangements of these elements in series and parallel. We compared the tensile properties of the bundles and their component filaments of commercial PET using an INSTRON® tensile tester and a MANTIS® single-fiber tensile tester. The tested values obtained when using the INSTRON® tester were compared with the expected values provided by the Peirce and Knox models by applying the data from the MANTIS® single-fiber tensile tester.

2. Experimental

2.1. Materials

To study the random breakage behavior of bundles, we prepared bundles from a different number of filaments of 262 denier(d)/12 filament(f) PET yarn provided by Kanebo Co. Ltd. Filaments having large denier could be separated readily from the yarn. All filament yarns were drawn from relatively restricted sections of the package, to avoid any large effects that might be encountered through the packages. Single filaments were separated from the raw filament yarn and artificially prepared into 1–12-filament bundles. We considered bundles to be parallel arrangements of component filaments that might behave independently from one another and filaments to be continuous chains of components of unit length. We selected lengths of 10, 20, 30, 40, 60, and 80 mm from twelve filament bundles. For the tensile tests of the bundles that were arranged in a series-parallel combination of filaments, we glued the specimens to a paper tab using a polyamide-epoxy resin. We considered N-filament bundles to be an arrangement of component filaments of PET yarn, as illustrated in Fig. 1, which exists in a continuous chain of components of unit length. We made the following basic assumptions for the series-parallel combination model:

1. No inter-filament friction exists in a bundle.
2. All filaments within a clamped bundle have equal length.
3. Filament axes are parallel to the extension and direction when the filament was clamped between the upper and lower gripper.
4. Filaments within a bundle are ideally clamped, permitting no filament slippage or damage at clamping points as a result of load concentration.

In a well-combed and brushed filament bundle, assumptions 1 and 3 should hold; assumption 2 is satisfied when bundles are glued at the same tension; assumption 4 should hold when a default specimen is checked after testing, which is a safeguard against the usual experimental errors that stem from the flawed clamping conditions. These assumptions provide a great simplification when studying large filament bundles and their tensile behavior. To investigate the relationship between

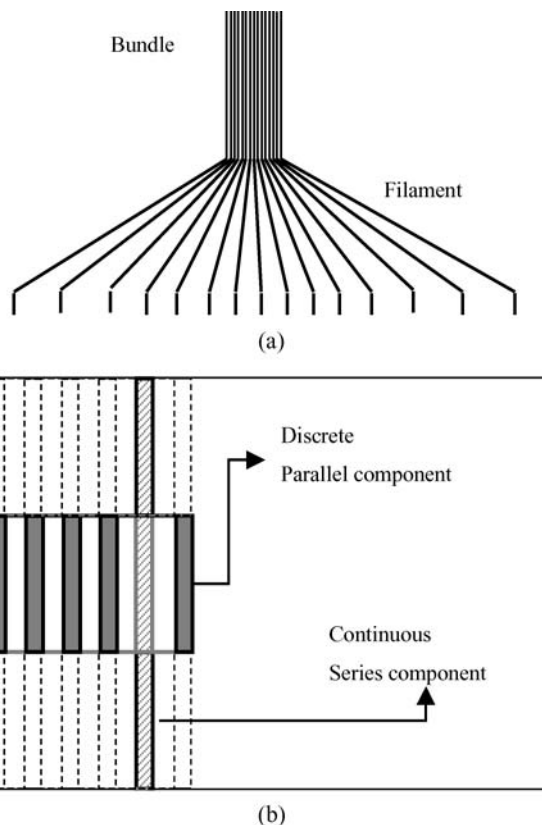


Figure 1 The series-parallel combination model of bundle strength: (a) bundle and filaments; (b) series-parallel combination.

the breaking strength of single filaments and bundles, we prepared four partially drawn yarns (DPY) that were 75d/36f and 50d/24f PET yarns. We performed single-filament tensile tests using a MANTIS® single-fiber tensile tester. The information achieved was stored in a computer database for subsequent analysis. The tensile tests of bundles were performed using an INSTRON® tester (Table I).

2.2. Measurements

2.2.1. Tensile test of N-filament bundle

The tensile tests of N-filament bundles were performed on an INSTRON® (model 4468, UK) tensile tester by using a 100-N load cell. Lengths of 10, 20, 30, 40, 60, and 80 mm were selected from each of twelve filament bundles, i.e., from a single-filament bundle to a twelve-filament bundle (Table I). The specimens were then mounted in clamps and tested at a cross-head speed of 60 mm/min. We performed a total of 720 tensile tests, which we repeated 20 times for twelve N-bundles of each gauge length. The data obtained from each test were treated as a set of breaking strengths and breaking

TABLE I The classification of PET samples

Sample name	Denier/filament	Company	Instrument
PET-A	262/12	Kanebo	Instron®
PET-B	75/36	Kolon	Instron® & Mantis®
PET-C	75/36	Hyosung	Instron® & Mantis®
PET-D	50/24	Kolon	Instron® & Mantis®
PET-E	50/24	Hyosung	Instron® & Mantis®

strains and were compared with those sample properties from other sets for filaments of the same PET yarns.

### 2.2.2. Tensile testing of a single filament

Single-filament tensile tests were performed using a MANTIS<sup>®</sup> single-fiber tensile tester (Zellweger Uster Inc.) having a 3.175-mm gauge length at a 60 mm/min extension rate, as given in Table I. We performed a total of 225 or 150 single-filament tests, which were repeated three times for each filament, on the MANTIS<sup>®</sup> for each filament type. The information was stored in a computer database for subsequent analysis. We acquired a large amount of data on the tensile properties of single filaments through MANTIS<sup>®</sup> single-filament tensile testing. The single-filament tensile properties included strength, elongation, modulus, work, and crimp. The modulus is defined as the ratio of the breaking strength to the breaking elongation. The work is defined as the total area under the load-elongation curve. The crimp is defined as the difference between the filament curvilinear length between the clamps and the gauge length expressed as a percentage of the latter. The single filament test used by the MANTIS<sup>®</sup> tester consists of two measurement modes: mechanical and optical. The filament was mounted automatically, i.e., the operator placed a filament across the jaw face and the filament was then straightened by the use of a vacuum pipe. To permit optical measurement, the filament was placed under a small stress (<0.2 g) at a fixed length of 3.175 mm. The filament was then radiated with an infrared light source, and a detector determined the attenuation of this light due to the filament diameter. A second detector measured the scatter of the light at an angle of 45° from the horizontal plane, as indicated in Fig. 2. After these measurements were performed, one end of the filament was released and the filament was relaxed for a short period of time before being clamped again at the pre-determined gauge length for the tensile tests.

### 2.2.3. Tensile testing of PET yarn on the INSTRON<sup>®</sup> tester

The specimens were prepared from 75d/36f (PET-B, PET-C) and 50d/24f (PET-D, PET-E) PET filament

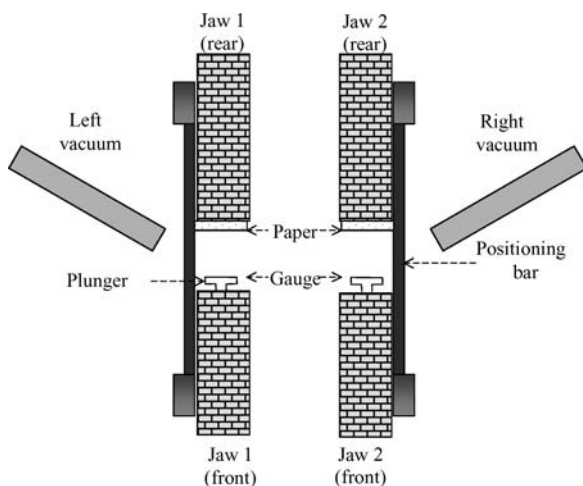


Figure 2 The MANTIS<sup>®</sup> single-fiber tensile tester.

yarns provided by Kolon Co. and Hyosung Co., Korea. Lengths of 10, 20, 30, 40, 60, and 80 mm were selected from each PET yarn. Paper tabs were glued to the ends of the specimen using a polyamide-epoxy resin. The prepared specimen was then tested on an INSTRON<sup>®</sup> (model 4468, UK) tensile tester by using a 10-N load cell. The specimen were then mounted in clamps and tested at a cross-head speed of 60 mm/min. Data obtained from each test were treated as a set and the breaking strengths, breaking elongations, and moduli were compared with those sample properties obtained from the data obtained using the MANTIS<sup>®</sup> single-fiber tester.

## 3. Results and discussion

### 3.1. The bundle strength of N-filament bundles

In this study, we prepared 1–12-filament bundles from 262d/12f yarn (PET-A). Fig. 3 provides the breaking behavior for the 1–12-filament bundles having different gauge lengths. As the load-extension curve of each bundle indicates, single filaments of each bundle broke at a constant load and the two-filament bundles broke perfectly at twice the load of the first breakage. According to further breaking experiments, the breaking point lost its clear-cut features, but a point of inflection remained. However, no trace in the load-extension curve remained. Consequently, the load is supported by all of the filaments when none of the filaments is broken. When one filament breaks and slips free, because there is no friction between the filaments, it no longer contributes to the strength of the bundle and the surviving filaments stand load one after another, and finally the system brakes abruptly. This force from the broken filament can be redistributed in many ways. It can be distributed to all surviving filaments (equal-load sharing) or it is possible that only the filaments adjacent to the broken filament support the load from the failed filaments (load-load sharing). In the latter case, the adjacent filaments support a much greater load than do the filaments that support only their own load. After only a few percent of the filaments in the bundle break, the entire bundle fails catastrophically. Fig. 4 displays a typical load-extension curve of N-filament bundles for 262d/12f PET filament yarn; this figure indicates that the bundle strength increased linearly with respect to the increase in the number of filaments, but the breaking extension does not display any significant relationship with this number. In the case the parallel bundles, no significant interactions occurred between adjacent filaments and so, for example, slack, slippage, and friction did not occur when the bundle was loaded. The breaking loads of the N-filament bundles integrally and linearly increased with the number of filaments, as indicated in Fig. 5, which displays the regression fit of the breaking strength as a function of the number of filaments. Fig. 5 displays that single filaments within a bundle were relatively independent and inter-filament friction had little effect in a bundle. Although the number of filaments increased, there was little change in the efficiency of the breaking

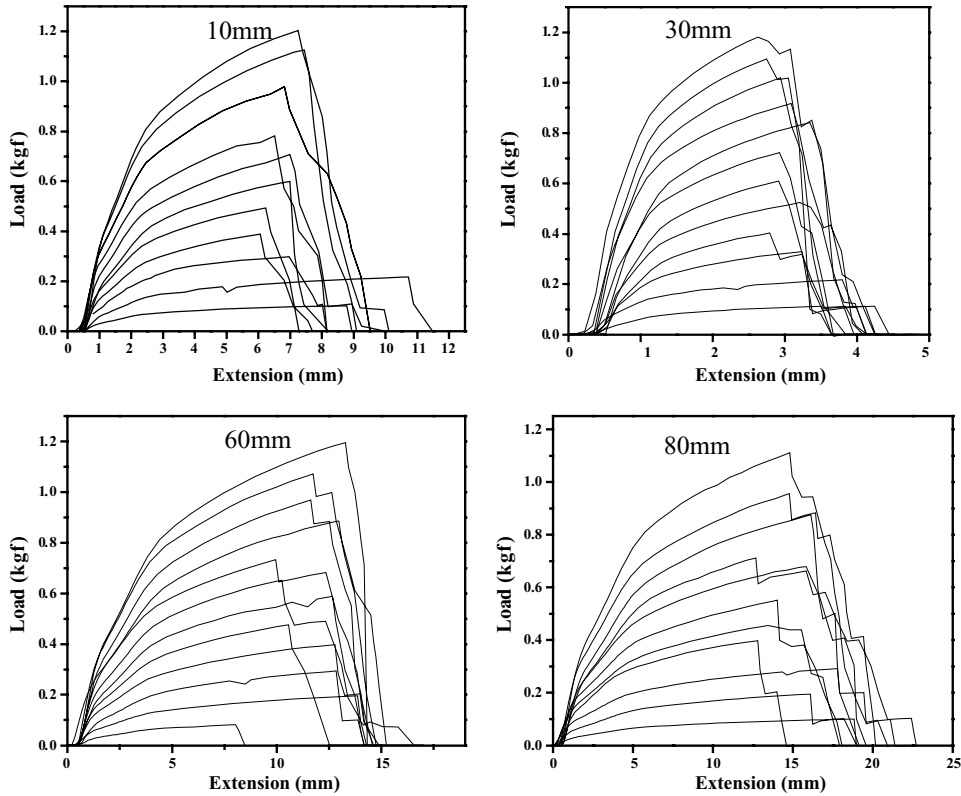


Figure 3 The load-extension curves of the 1–12-filament bundles for the 262d/12f PET yarn at different gauge length.

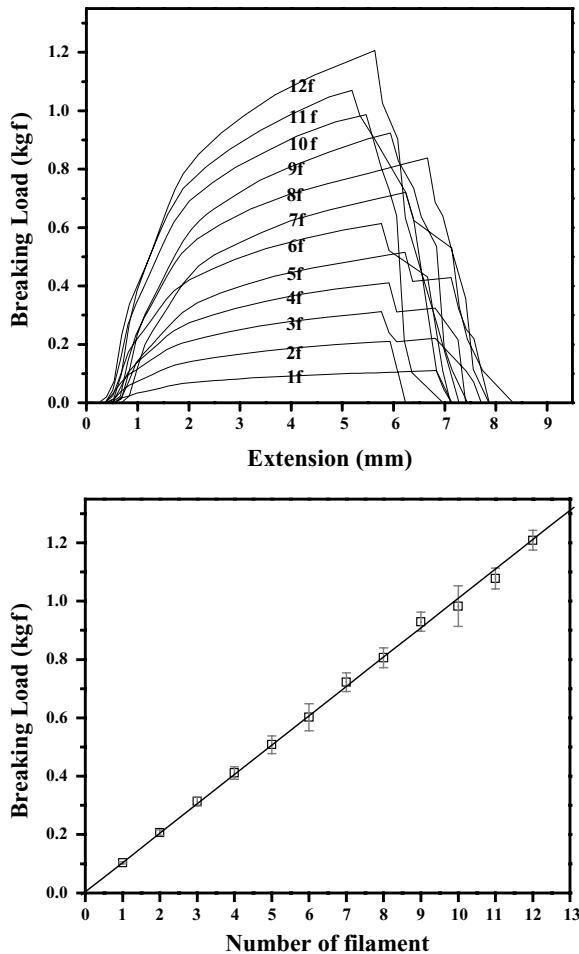


Figure 4 The breaking load and linear regression fit of the 1–12-filament bundles at 20-mm gauge lengths for the 262d/12f polyester yarn.

strength at maximum load. The efficiency of the breaking strength at breaking load decreased exponentially, however, because the load concentration increased on adjacent filaments upon increasing the number of filaments and then failure occurred catastrophically. Fig. 6 illustrates the weakest-link effect and bundle size effect of the N-filament bundles. As the length of a specimen increased, the probability of the existence of defects should increase. However, there was no significant effect when compared to the effect of the bundle size, i.e., the number of filaments. Therefore, we believe that the major effects that determine the bundle strength are the number of filaments and the load sharing behavior of the single filaments constructed into that bundle.

### 3.2. The strength of single filaments and bundles

We measured the breaking strength of PET single filaments by using a MANTIS<sup>®</sup> single-fiber tensile tester and the bundle strength of PET yarn by using an INSTRON<sup>®</sup> tensile tester. The measured strength data of the single filaments were compared with the bundle strength of the PET filament yarn. As mentioned above for the results of testing a single filament, the breaking strengths of the single filaments were distributed normally when conducted using MANTIS<sup>®</sup> tests. It remained doubtful, however, whether or not the bundles of PET filaments had normal distributions, because the bundles displayed wholly different behavior. Therefore, we needed to determine whether the tensile properties of the bundles were similar to those of the

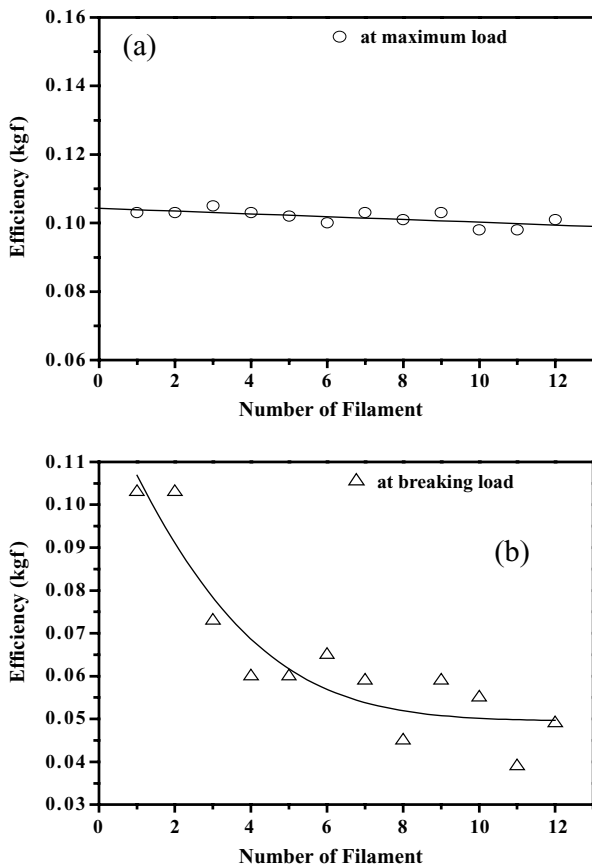


Figure 5 The efficiency of the breaking strength of the 1–12-filament bundles for the 262d/12f PET filament yarn: (a) at maximum load; (b) at breaking load.

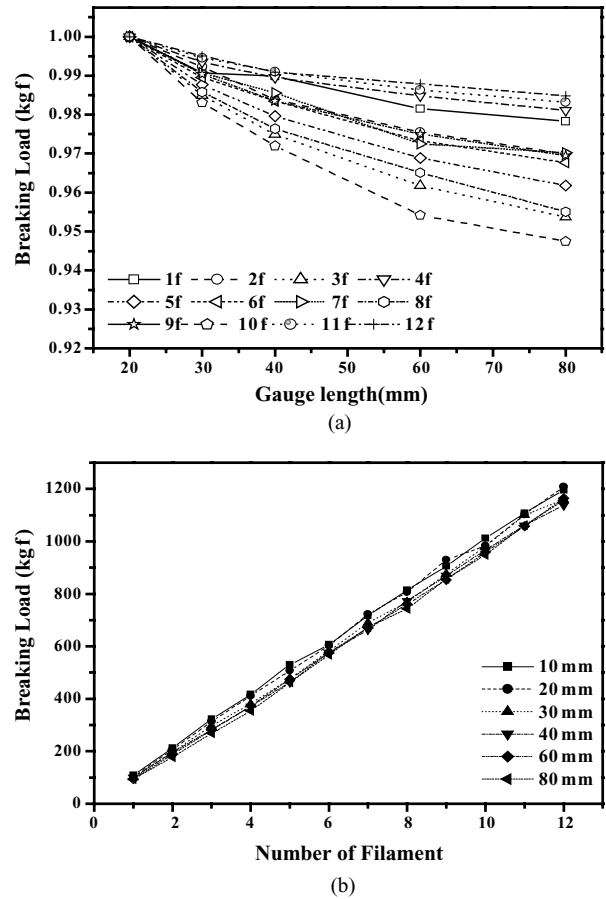


Figure 6 The weakest-link and bundle size effects of the 1–12-filament bundles for the 262d/12f PET filament yarn.

single filaments. In addition, we compared the results obtained for PET filament yarns prepared by different spinning techniques. PET-B possessed a similar probability distribution function (p.d.f.) to that of PET-C, but a different p.d.f. to that of PET-C in filaments. With regard to the hazard function, the PET-B yarn appeared to have a higher slope than did the PET-C yarn, but its tendency was reversed in filaments. This finding provides evidence that the breaking strength of the PET-B filament was higher than that of the PET-C filament, even though the breaking strengths of PET-B yarn and PET-C yarn were similar. Therefore, we conclude that a bundle's strength is determined by the strength and arrangement characteristics of its component filament. In 50d/36f PET yarn, the bundle strength gave different values of p.d.f., in location parameter, even though two of the yarns appeared to have similar breaking strengths in their single-filament states.

### 3.3. Comparison of the tested and expected values

We compared our tested values with the values expected from calculations using Peirce's theory and Knox's hazard function. From the breaking strength data tested by the MANTIS<sup>®</sup> single-fiber tester, we acquired the mean and standard deviation of the breaking strength, and then in-putted these values into the Peirce's equation. The second expected value was acquired from the hazard function described by Knox.

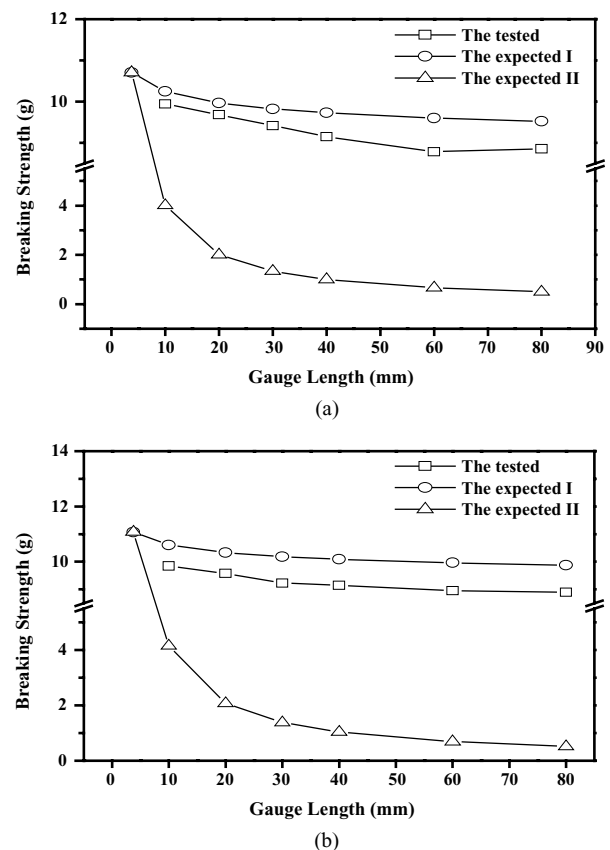
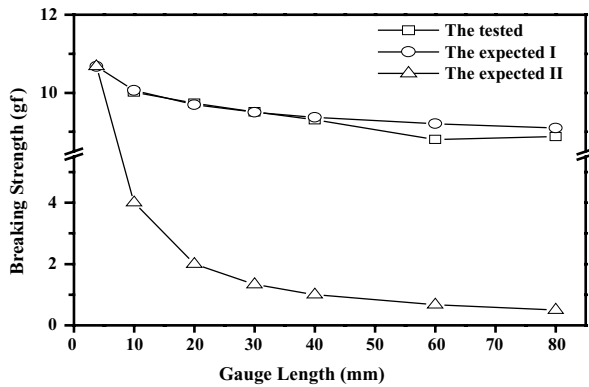
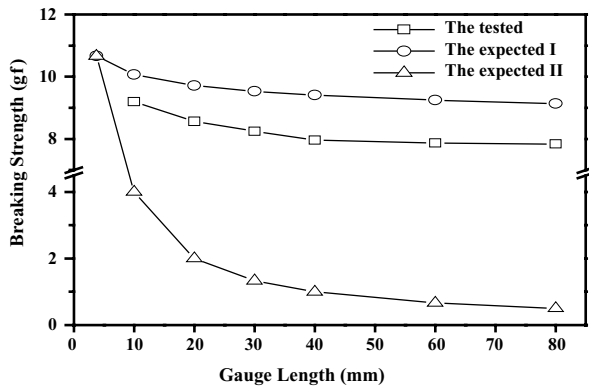


Figure 7 Comparisons between the tested values obtained using INSTRON<sup>®</sup> and the expected values obtained using MANTIS<sup>®</sup> for the 75d/36f PET single filaments: (a) PET-B; (b) PET-C.

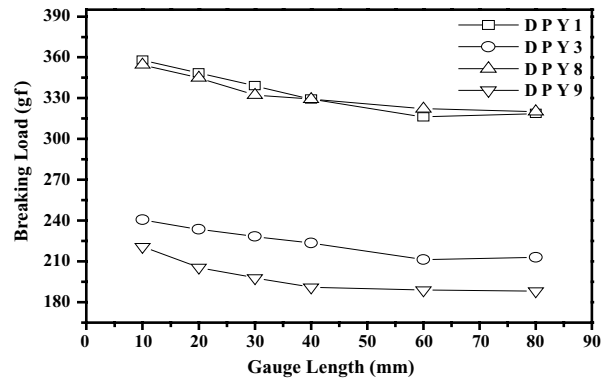


(a)

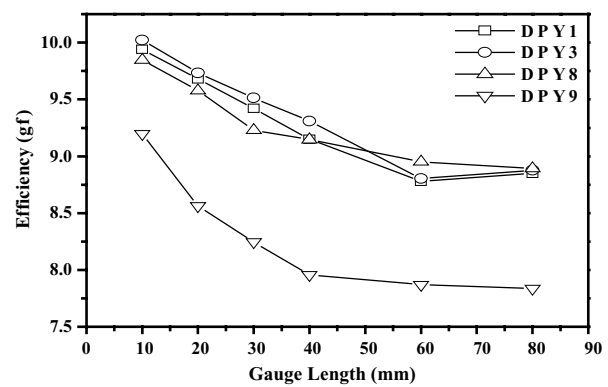


(b)

Figure 8 Comparisons between the tested values obtained using INSTRON<sup>®</sup> and the expected values obtained using MANTIS<sup>®</sup> for the 50d/24f PET single filaments: (a) PET-D; (b) PET-E.



(a)



(b)

Figure 9 The effects that length and bundle size have on the breaking strength of commercial PET yarn: (a) the breaking load; (b) the efficiency.

The results are presented in Figs 7 and 8, which indicate that the expected values obtained using Peirce's theory are better approximations of the tested values than are those predicted by the hazard function. The expected values obtained using Peirce's theory, however, also present a number of differences in relation to the tested plots. Consequently, we conclude that the PET filaments followed a normal distribution because Peirce assumed the breaking strength of a filament to be normally distributed. Fig. 9 illustrates the effects that the length and bundle size have on the breaking strength of commercial PET yarn. Fig. 9a indicates that the breaking load of the PET filaments decreased as the gauge length increased, i.e., the weakest link theory. Fig. 9b displays a plot of the efficiency of commercial PET filament yarn. For PET-B, PET-C, PET-E was appeared the similar scale with the exception of PET-D. Despite having the same denier, the filaments displayed different behavior. This finding indicates that the difference is due to the load sharing breakage. The load sharing behavior on the random breakage of PET bundles is very complicated because of the effects of slippage and friction between adjacent filaments; these effects are more significant in small-denier filament bundles.

**4. Conclusions**

In this study, we prepared N-filament bundles from 262d/12f PET filament yarn to investigate the behavior of the random breakage of a bundle; we com-

pared these results with those obtained using a commercial PET filament yarn. We compared the breaking strengths determined by MANTIS<sup>®</sup> tests with those from INSTRON<sup>®</sup> tests. In addition, we evaluated the strength of both filaments and bundles by using the MINITAB statistic package. The normality tests for PET filaments indicated that commercial PET single filaments and prepared N-filament bundles followed normal distributions and that the bundle strength could be predicted from the distribution function of each single filament of PET yarn. The results of N-filament bundles are explained by the weakest-link effect and the bundle size effect of the N-filament bundles. That is to say, although when the length of a specimen increases, the probability of the existence of defects should also increase, but we found that the major effects that determining the bundle strength are the number of filaments and the load sharing behavior of each single filament. In a comparison between the expected and tested values in the PET filaments and bundles, Peirce's theory provided a better fit than did a simple hazard function. Consequently, in both series and parallel effects, we found that the breaking strength of a bundle was influenced by the length effect (the weakest link theory), but the load-sharing behavior of the component filaments in a bundle had a greater effect on the bundle strength. We implicate that the load sharing behavior has an effect on the random breakage of a polyester bundle because slippage and friction between adjacent filaments have more significant effects in small-denier filament bundles. For further study, it is worthwhile

investigating how much effect the slippage and friction have on the load-sharing behavior of the random breakage of the bundles.

## References

1. F. T. PEIRCE, *Text. Res. J.* **17** (1926) 355.
2. B. D. COLMAN, *J. Mech. Phys. Solids* **7** (1958) 60.
3. H. C. CHEUNG, *Text. Res. J.* **34** (1964) 597.
4. M. W. SUH, A Study of the Distribution and Moments of Bundle Strength in Sequential Breakage of Parallel Filaments, Doctoral Thesis (North Carolina State University, 1969).
5. P. K. SEN, B. B. BHATTACHARYYA and M. W. SUH, *Ann. Statist.* **1** (1973) 297.
6. L. J. KNOX and J. C. WHITWELL, *Text. Res. J.* **41** (1971) 510.
7. L. J. KNOX, J. C. WHITWELL and M. J. HUTZ, *Text. Res. J.* **42** (1972) 688.
8. S. L. PHOENIX and H. M. TAYLOR, *Adv. Appl. Prob.* **5** (1973) 200.
9. S. L. PHOENIX, *Fiber Sci. Tech.* **7** (1975) 15.
10. S. L. PHOENIX, *Int. J. Eng. Sci.* **13** (1975) 287.
11. R. E. PITT and S. L. PHOENIX, *Text. Res. J.* **52** (1982) 408.
12. S. L. PHOENIX, *Text. Res. J.* **49** (1979) 407.
13. R. P. NACHANE and K. R. KARISHNA, *Text. Res. J.* **50** (1980) 639.
14. N. PAN, *Text. Res. J.* **62** (1992) 749.
15. N. PAN, *J. Mater. Sci.* **28** (1993) 6107.
16. N. PAN and R. POSTLE, *J. Text. Inst.* **86** (1995) 559.
17. T. NAKASHIAMA and K. OTA, *Text. Mach. Soci. Jpn.* **18** (1965) 60.
18. P. E. SASSER, F. M. SHOFNER and Y. T. CHU, *Text. Res. J.* **61** (1991) 681.
19. M. C. RAMESH, R. RAJAMANICKAM and S. JAYARAMAN, *J. Text. Inst.* **86** (1995) 459.
20. H. E. DANIEL, *Adv. Appl. Prob.* **21** (1989) 315.
21. J. W. S. HEARLE, P. GROSBEG and S. BACKER, in "Structural Mechanics of Fibers, Yarns, and Fabrics" (John Wiley & Sons, New York, 1969).
22. H. J. KOO, S. H. JEONG and M. W. SUH, *Fibers and Polymers* **2** (2001) 22.

Received 5 October 2004  
and accepted 14 February 2005